EUROPEAN ACADEMIC RESEARCH
Vol. VII, Issue 6/ September 2019

Impact Factor: 3.4546 (UIF)
DRJI Value: 5.9 (B+)

ISSN 2286-4822
www.euacademic.org

Applying (A.I) Algorithms to Stabilize the Cooling State in a 3-Dimension Continuous Casting Process

MUHAMMAD NAEEM
NAVEED SHEIKH
Department of Mathematics
University of Balochistan, Quetta, Pakistan
MUDASSAR IQBAL
Department of Mathematical Sciences
Balochistan University of Information Technology, Engineering and Management Sciences (BUITEMS), Quetta, Pakistan
MUHAMMAD ASIF
DURDANA MUNIRAND
SAMINA NAZ
Department of Mathematics, University of Balochistan
Quetta, Pakistan

Abstract

In this research, we introduce a method for re-establishing the cooling state in a crystallizer and furthermore in a cooling zone of 3-dimensional continuous casting process. Generally, the shape of the cooling system changes the quality of the cast produced. That is why it is necessary to choose suitable conditions for cooling of metal ingots. The inverse problem studied, which involves explaining the method of the continuous casting process. The formulated problem, the Stefan's, the condition was removed and the isotherms were found as the interface where the solidification temperature seems to be same, results are obtained depending upon the steadiness of solution and Tikhonov Regularization's, convergence.

Keywords: Heat transfer, Artificial intelligence, Continuous casting, the inverse problem

1 INTRODUCTION

Casts are commonly produced via a continuous casting method. The efficiency of the cast depends on the design (quality) of the system (Słota, 2009; Hetmaniok et al., 2015). It is important to develop an effective method for an optimal cooling strategy that focuses on secondary cooling zones with constant casting velocity (Nawrat et al., 2009). This method of the continuous casting process utilizes the heat transfer coefficient in secondary cooling zones. Major studies have focused on generic algorithms for two-dimensional problems and there is an increasing need to focus on the three-dimensional models.

Assuming that the heat is only transferred in the way that is orthogonal to the axis of casting, the temperature field will be considered to be pseudo-steady and generated when the operational cycle of the casting element is undisturbed. Considering this thermal symmetry while assuming that the casting domain (D) is constructed of 2 sub-domains into the liquid (D1) and the solid (D2) phases, which is distinguished by a freezing point (Γg), the two-phase Stephan will effectively describe heat exchanging process "(pseudo steady temperature field)" and the "(freezing front place)" (Vasil'ev, 2001). There are other parameters for continuous casting other than the cooling conditions that need to be determined and they include inverse geometric problem (phase change phase location) and thermal resistance and heat transfer coefficient of the mold (space between the ingot and crystallizer) (Constalas et al., 2002; Nowak et al., 2002).

(Rogers, Berger, & Ciment, 1979) presented a numerical solution of heat conduction. The numerical solution used for this method of two-phase alternatively. (Engl & Langthaler, 1985) describes the process of solidification in the casting of steel for external cooling and using the casting speed. They describe a method based on non-linear optimization to evaluate these control variables in such a way that a pre-calculated set of solidification is approximated with sufficient accuracy. (Langthaler, 1987) computes the Inverse problem of the nonlinear heat equation and prove its uniqueness, existence, and continuous dependence. (Binder, 1990) presented a parabolic equation(nonlinear) which describes the models in continuous casting of the slab for secondary cooling of steel and provide stability results of problems to the both of determining

solidification with Cauchy data and inverse problem for cooling technique leads to a formulated solidification front. The convergence of Tikhonov regularization and Stability are also proved. (O'Mahoney, & Browne, 2000) presented a method to calculate thermal boundary conditions for continuous casting process during solidification. (Chakraborti, N., Kumar, R., & Jain, D., 2001) describes in their paper that most useful device in the industry of casting process is made using steady heat transfer and PCGA. (Cheung, N., & Garcia, A., 2001) used the process of continuous casting have connected between Artificial Intelligence and a numerical heat transfer flow.

(Santos, Spim, Ierardi, & Garcia, 2002) presented algorithms which directly search methods in the forging industry. Because Casting process is controlled by various parameters such that casting speed, steel composition, casting temperature, etc. (Santos, Spim, & Garcia, 2003) presented and introduced an algorithm (software) for controlling the conditions of the casting process. (Chakraborti, Gupta, & Tiwari, 2003) discussed the detailed study of the casting process at optimization level genetic algorithm biologically. (Dorigo, & Stützle, 2003) discussed the properties of ACO algorithms, by theoretically & experimentally. (Nawrat, & Skorek, 2005) presented their work to show the technique to find out the unknown thermal resistance by the help of temperature at the number of sensors fixed in the mold. (Santos, Garcia, Frick, & Spim, 2006) studied heat transfer coefficients during casting of the week and average carbon steels by casting parameters. (Karaboga, & Basturk, 2007) discussed swarm intelligence like an ant colony, Bee colony and a flock of birds systematically organized. (Słota, 2008) explained an algorithm for the Stefan problem of the two-phase inverse problem. (Słota, 2009) also explained function with the boundary conditions along both cooling zones in the two and three dimensions continuous casting processes respectively.

(Nowak, Smolka, & Nowak, 2010) presented a 3-D solution numerically for the inverse boundary problem of a continuous casting process of an aluminum alloy. (Słota, 2011 and Hetmaniok, Słota, Zielonka, 2011) described the reconstruction of heat flux and heat transfer coefficient in solidify pure metals and Applied in swarm intelligence algorithms to solve the inverse problem of heat conduction. (Hetmaniok, Słota, Zielonka, & Pleszczyński, 2013) shown

usage of an algorithm of Artificial Bee Colony in a solution of inverse-problem in continuous casting consists of the reconstruction of suitable parameters characterizing the cooling conditions in crystallization and secondary cooling zone. (Hetmaniok, Słota, & Zielonka, 2015) the proposed solution of the 2-D inverse problem for the continuous casting process.

The remaining paper is formulated as follows. Section 2 is a formation of the problem for 3 phase Stefan conditions. Section 3 deals with the development of proposed algorithms taken from artificial intelligence. In Section 4, numerical examples have been evaluated using suitable demonstrations. Section 5 summarizes the contributions and concludes the paper

2 PROBLEM FORMATION

Here we discussed continuous casting, running in the uninterrupted cycle in a device vertically assembled; consider that heat transfer happens just toward the path opposite to the axis of casting. We assume a pseudo-steady temperature field by creating throughout the uninterrupted functional cycle of the casting furnace. In our suppositions, the thermal equilibrium, the casting's area "D" might be divided as an area made out of two subdomains, D_1 known as the liquid phase and D_2 known as the solid phase), divided by the freezing front. In these areas, coordination of space (see Fig-1), the procedure of heat exchange, including the pseudo-steady temperature field and the location of the freezing front is portrayed by the 3 phase Stefan problem.

Suppose $D = [0, b] \times [0, d] \times [0, z^*]$ for the 3 Dimensional problem.

Expressing 3-D problem (on an x-y-z plane) as:

$$D = [0, x] \times [0, y] \times [0, z]$$

The boundary domain D for 3-D problem is described by 7 equations (Fig- 1):

$$\mathbb{\Gamma}0\ (3 - D\ problem) = \{(x, y, 0);\ x\epsilon\ [0, b], y\epsilon\ [0, d]\}$$
$$\mathbb{\Gamma}1\ (3 - D\ problem) = \{(0, y, z);\ x\epsilon\ [0, d], y\epsilon\ [0, z*]\}$$
$$\mathbb{\Gamma}2\ (3 - D\ problem) = \{(x, 0, z);\ y\epsilon\ [0, b], z\epsilon\ [0, z*]\}$$
$$\mathbb{\Gamma}3\ (3 - D\ problem) = \{(b, y, z);\ y\epsilon\ [0, d], z\epsilon\ [0, z1]\}$$

$$\mathbb{\Gamma}4\,(3-D\ problem) = \{(b,y,z);\ y\epsilon\,[0,d], z\epsilon\,[z1,z*]\}$$
$$\mathbb{\Gamma}5\,(3-D\ problem) = \{(x,d,z);\ x\epsilon\,[0,b], z\epsilon\,[0,z1]\}$$
$$\mathbb{\Gamma}6\,(3-D\ problem) = \{(x,d,z);\ x\epsilon\,[0,b], z\epsilon\,[z1,z*]\}$$

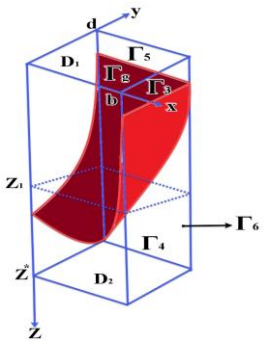

Figure 1: Schematic illustration of the domains (D) used for all Stefan's 3-D problem equations

In the continuous casting process, the selection of cooling conditions is value-based as follows:

$$T_2\,(r_i) = U_i \qquad i = 1, 2, \ldots, N$$
$$r_i \in D_2$$

Where $r_i = (x_i, z_i)$ for 2D problem, $r_i = (x_i, y_i, z_i)$ for 3D problem, N = number of measurements.
On freezing front,

$$\mathbb{\Gamma}_g = c_k\, g_k\, w \frac{\partial T_k}{\partial z}\,(r) = k_k \nabla^2 T_k(r) \qquad r \in D_k, k = 1,2$$

Where:
$T_k = Temperature\ distributions\ in\ domains$,
$D_k\,(k = 1,2), w = casting\ velocity,$
$c_k = specific\ heat\ for\ liquid\ phase\ (k = 1)\ and\ solid\ phase\ (k = 2),$
$g_k = specific\ heat\ and\ mass\ density\ for\ liquid\ phase\ (k = 1)\ and\ solid\ phase\ (k = 2)$
$k_k = thermal\ conductivity\ for\ liquid\ and\ solid\ phases\ (k = 1\ \&\ k = 2).$

The boundary condition for ($\mathbb{\Gamma}_0$) in two cases is determined based on

pouring temperature ($T_Z > T^*$)

$$T_1(r) = T_z \quad r \in \mathbb{\Gamma}_0$$

The boundary ($\mathbb{\Gamma}_1$) in the 2-D problem occurs as $\mathbb{\Gamma}_1 U \mathbb{\Gamma}_2$ in the 3-D problem. The boundary condition is homogeneous and it is expressed as:

$$\frac{\partial T_k}{\partial n}(r) = 0 \qquad r \in \mathbb{\Gamma}_1 \quad (or \quad r \in \mathbb{\Gamma}_1 \cup \mathbb{\Gamma}_2)$$

The casting mold $\mathbb{\Gamma}_3$ in 2-D problem occurs as $\mathbb{\Gamma}3U\mathbb{\Gamma}5$ in the 3-D problem. The boundary condition is expressed as:

$$-k_k \frac{\partial T_k}{\partial n}(r) = q(r) \qquad r \in \mathbb{\Gamma}_3 \quad (or \quad r \in \mathbb{\Gamma}_3 \cup \mathbb{\Gamma}_5)$$

The secondary cooling zone is $\mathbb{\Gamma}_4$ in the 2-D problem and occurs a $\mathbb{\Gamma}4U\mathbb{\Gamma}6$ in the 3-D problem. Its boundary condition is expressed as:

$$-k_k \frac{\partial T_k}{\partial n}(r) = h(r)[T_k(r) - T_\infty] \qquad r \in \mathbb{\Gamma}_4 \quad (or \; r \in \mathbb{\Gamma}_4 \cup \mathbb{\Gamma}_6)$$

In the above equation, h = heat transfer coefficient, T_∞ = Surrounding temperature

The conditions for temperature continuity and Stefan problem for freezing Front ($\mathbb{\Gamma}_g$) is expressed as:

$$T_1(r) = T_2(r) = T^* \qquad r \in \mathbb{\Gamma}_g$$

$$L\, Q_2\, v_n = -k_1 \frac{\partial T_1(r)}{\partial n}\Big| + k_2 \frac{\partial T_2(r)}{\partial n}\Big|_{T_g}$$

In the above equation,

$T* = Melting\ point\ temperature,$

$L = Latent\ heat\ of\ solidification,$

$v_n = freezing\ front\ velocity\ (normal\ direction\ vector)$

The continuous cast mold is characterized by heat flux whereas the secondary cooling zone is strongly affected by the heat transfer condition. The heat flux and heat transfer coefficient can compute as follows:

$$f(r) = \begin{cases} q_3(r) & r \in \mathbb{\Gamma}_3 \\ h_4(r) & r \in \mathbb{\Gamma}_3 \end{cases}$$

In the above expression, the f(r) function is a designate of the 2-D problem and it is extrapolated in the 3-D problem as follows:

$$f(r) = \begin{cases} q_3(r) & for \quad r \in F_3 \\ q_5(r) & for \quad r \in F_5 \\ h_4(r) & for \quad r \in F_4 \\ h_6(r) & for \quad r \in F_6 \end{cases}$$

Assuming that the f(r) function is a steady form, the following equations are adopted for the 3-D problem:

$$c_k \, g_k \, w \frac{\partial T_k}{\partial z} \, (r) = \, k_k \nabla^2 T_k(r) \qquad r \, \in \, D_k, k = 1,2$$

$$L \, Q_2 \, v_n = \, -k_1 \frac{\partial T_1(r)}{\partial n} \Big| + k_2 \frac{\partial T_2(r)}{\partial n} \Big|_{T_g}$$

In the above 2 equations, the temperature values, $T_i \, = \, T_2 \, (r_i)$ which corresponds to f(r) function

Assuming that temperature (U_i) is given as actual temperature whereas this simulation (algorithm) generates the virtual temperature (T_i), then model error determined as:

$$J(f) = \, \|T - U\|^2 + \gamma \|f\|^2$$

In this equation γ functions as a regularization parameter whereas $\|T - U\|^2$ is equivalent to $\sum_{i=1}^{N} (T_i - U_i)^2$and $\|f\|^2$ is equivalent to$\int_S \, \omega(r)[f(r)]^2 dS$; where ω(r) = weight function,

$S \, = \, \Gamma 3 \, U \, \Gamma 4 \, U \, \Gamma 5 \, U \, \Gamma 6$ for 3-D problem and r = point of the surface denoted as S.

It is important to understand the solutions of the complete 2 phase inverse Stephan problem and the 2 phase, 3D inverse Stephan problem. Two main constants (values) to consider include time heat flux values, solidification time in successive cooling zones, and heat transfer coefficients along the secondary cooling zones (Nawrat and Skorek, 2005).

3 METHODOLOGY

From the second section, the suggested methodology needs 2 steps:

1) The solution of direct Stefan problem

2) Narrowing functional that defines approximate solution error.

The finite difference method, by using the alternating phase truncation method, is used for the solution of direct Stefan problem. In this proposed method, enthalpy is used in replacement of the temperature. Both stages are executed for the computation of each step. The entire region is minimized from the first step to the second step (liquid to the solid phase). Two A.I optimization algorithms that are the ACO and PSO algorithms, which are used to reduce the functional by obtaining the outputs.

3.1 ACO Algorithm

It is related to the "Swarm Intelligence Algorithms", which is described by partitioning issues into shorter functions that are completed from specific individuals. Now entire species of ants belong to the ACO don't have awareness of the entire problem. It is necessary to accomplish their own given duties by pursuing very easy principles and suitable interactions among the individuals which lead to the solution.

In this ACO algorithm, ants' colonies search for food. The blind ants exchange information to each other spreading a chemical liquid known as a pheromone. One ant drops pheromone on the land after searching food source, this may be discovered and identified by the remaining ants. This common smell influences alternate ants to pursue pheromone left-behinds. Trail of pheromone develops intense gradually, more ants will pursue the track. Given technique enables the smallest way to be acquired quickly by ants if two ways are accessible, and resultantly pheromone track increased quickly. Pheromone dissipates after a while fades more quickly on the extended way in respect to the smallest way.

By applying the ACO algorithm, the populated artificial ants shown in the vector form: $x_i;\ i \in [1, m]$, in the given domain should be chosen unevenly. An ant is selected as the best i-e x^{best} to reduced J function have the smallest value. Placement vector x^{best} enhanced from successive assessments by the algorithm, given that minimized objective function's, value with the vector discovered. Particularly, the ACO processed in the following way:

I. Revising the positions of ants:

- Casually chose dx_i the vector that is:

$$-\beta_k \leq dx_i^j \leq \beta_k$$

(Where reduction parameter $\beta = \beta_0$ is described in the start of the algorithm, d means dimension and k means No. of the current iterations).

- Creating the new population ants

$$x_i = x^{best} + dx_i \ , i \in [1, m\}$$

II. Find & locate the best ant x^{best} from given populated ants.

III. Repeat Steps I and II, 12 times by assuming parameter step I.

IV. Reducing the range of dislocation of ants:

$\beta_{k+1} = (0.1)\,\beta_k$, used to stimulates the common vanishing of the pheromone leftover.

V. Repeat Steps I–IV, 1 time.

3.2 Particle Swarm Optimization

Particle Swarm Optimization has broadly used in "Artificial Intelligence Optimization" technique. It depends on the behaviour of the flock of birds and a pool of fishes for searching for food. Shi and Eberhart have been presented the fundamental work on PSO. It is based on the population search technique. In this method, particles are unevenly created to make the population. The particles are not discarded unlike in Genetic Algorithm. The movement of particles, searching for the optimal solution, is seen in the multi-dimensional space.

A particle defines a potential solution to the optimization problem. The particles are moved by their velocity. The particle velocity is computed as:

$$V_{id} = w \times V_{id} + c_1 \times rand\,() \times (P_{id} - X_{id}) + c_2 \times rand\,() \times (p_{gd} - X_{id})$$

$$Xid = X_{id} + V_{id}$$

Here

$V_{id} = velocity\ of\ particle$

$w = inertia\ weight$

$c_1, c_2 = constants$

$P_{id} = individual\ best\ position$

$P_{gd} = global\ best\ position$

$Xid = current\ particle\ position$

$rand\ () = function\ to\ generate\ random\ value$

The moving particles in every direction of space taking into consideration the last individual best location, it had visited earlier and the best location visited any of them. For local and global search, the small and large inertia weight is used. It shows more global search capability at the start of the run while having a more local search at the end of the run. By using linearly minimizing the inertia weight from relatively large value to a small value through the course of the run.

Here PSO has stopping criteria depends on the convergence of particles or a specific number of iterations (or if the best global does not affect from a certain number of iterations). Suitable inertia weights and constants are important for the maximum result of PSO. PSO has been applied to optimize reactive power flow in different standard and real electrical power systems.

4 RESULTS AND DISCUSSION

In this section, we consider 3 dimensional analysis of continuous casting of aluminium, presented by conditions given below:

$B = 0.1\,m, k_1 = k_2 = 390\,W/m\,K, d = 0.08\,m,$

$c_1 = c_2 = 410\,J/kg\,K, q_1 = q_2 = 9{,}000\ kg/m^3,$

$L = 210{,}000\,J/kg,$

$w = 0.002\,m/s, T* = 1{,}376\,K, T\infty = 343\,K$ and

$Tz = 1{,}500\,K.$

The following functions can be considered for exact cooling conditions:

$$q_3(z) = 450{,}000,\ h_4(z) = 4{,}500$$

Following function is designated for the set of constraints:

$$Vf = \{f(z):\ q_3 \in [350{,}000, 500{,}000],\ h_4 \in [4{,}000, 6{,}000]\}$$

It is expected in the calculations that there are four thermocouples in the said area. The distance between thermocouples and nearest domain boundary is 10 mm. From each thermocouple, successively, we have calculated: 10, 25, 50, and 100 temperature measurements. The successive estimations and spans along z-axis

are $\{0.02\ m, 0.008\ m, 0.004\ m, 0.002\ m\}$. The exact temperature values are utilized for calculations and these are weighed down the random error of normal distribution scaling with 1% & 2%.

The finite difference method is utilized for the alternating phase truncation approach, the estimations made on the grid of discrimination intervals equivalent to $\Delta z = 0.00004$, $\Delta x = b/100$, and $\Delta y = d/100$. Additionally, for this situation, a reasonable difference in the grid density didn't essentially affect the outputs acquired.

In table 1 and 2, reconstruction results of the boundary conditions are displayed by percentage errors relative. In the last two columns, the S.D "r" and the value of S.D "r^p" described in the mean value percentage are calculated, a number of measurement points are the boundary conditions for correct input data. The output from this principle appears for fifty measurements with 2% perturbations when the obtained outputs are placed nearer to each other than of hundred measurements with same perturbation.

Table 1. Calculated Results of 10 & 25 measurements

Perturbation	f	e [%]	r	r^p [%]
10 Measurement				
0%	450,396.257	0.08806	98.415312	0.021861
	4,500.82	0.018222	0.642211	0.014329
	449,957.62	0.009417	106.7892	0.023721
	4,462.74	0.82000	0.650604	0.014516
1%	449507.27	0.109496	3,089.21	0.686473
	4,509.67	0.214888	10.783001	0.240184
	450,516.62	0.114804	2,309.465	0.513241
	4,469.27	0.682888	4.547512	0.123567
2%	449,541.52	0.101884	134.9528	0.029995
	4,490.27	0.216222	3.422277	0.076085
	450,270.65	0.060144	49.381211	0.010975
	4,505.64	0.111111	1.80527	0.040207
25 Measurement				
0%	450,961.64	0.213698	68.929254	0.015309
	4,496.41	0.79777	0.184828	0.004101
	449,507.61	0.109420	94.477185	0.020983
	4,515.27	0.339333	0.267998	0.005948
1%	450,961.47	0.43659	1901.1172	0.422011
	4,495.45	0.101111	0.629522	0.013997
	450,017.64	0.003878	3,079.9541	0.683690
	4,499.56	0.009778	5.661122	0.125873
2%	450,543.57	0.120793	2,831.9755	0.628879

	4,456.64	0.963556	5.108147	0.114226
	450,097.52	0.021671	2606.8701	0.578892
	4,487.27	0.282889	4.588329	0.102602

Table 2. Calculated Results of 50 & 100 measurements (same notation from Table 1)

Perturbation	f	e [%]	r	r^p [%]
50 Measurement				
0%	380,006.45	0.001697	70.085891	0.018444
	4,000.81	0.020249	0.572247	0.014293
	379,961.85	0.010039	61.823345	0.016269
	4,006.61	0.0165250	0.405886	0.010138
1%	380016.41	0.004318	609.44958	0.160373
	3,981.54	0.0461500	1.452237	0.036374
	380,025.43	0.006692	308.427984	0.081161
	4,003.56	0.088999	0.507471	0.012710
2%	380,012.96	0.003411	104.617215	0.027531
	3,987.64	0.309000	0.383947	0.009611
	379,990.45	0.002513	69.275481	0.018230
	4,002.39	0.059749	0.357379	0.008946
100 Measurement				
0%	379,995.56	0.001168	98.583445	0.0253943
	4,008.24	0.205999	0.227905	0.005699
	380,011.44	0.003011	102.785432	0.027049
	3,989.67	0.0258249	0.141405	0.003536
1%	379,896.23	0.027308	60.195681	0.015843
	3,992.79	0.180250	0.443598	0.011104
	38,0005.24	0.001379	103.62598	0.027273
	3,996.84	0.078999	0.596254	0.014926
2%	380,015.67	0.004124	1885.2175	0.496111
	3,992.47	0.188250	1.649872	0.041267
	379,981.45	0.004882	1180.9025	0.310765
	4,003.54	0.088499	0.950432	0.023773

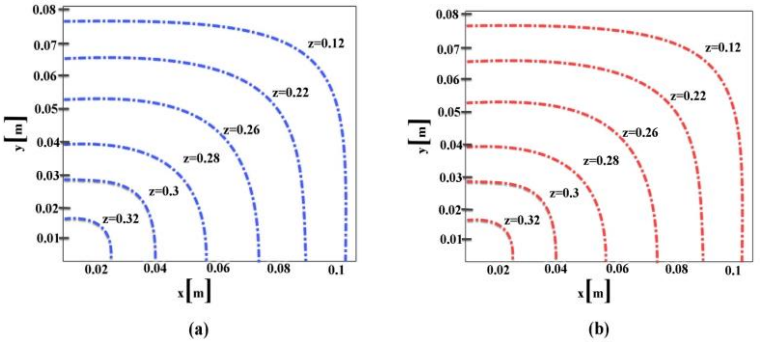

Figure 2. The dotted line shows reconstructed positions of freezing front for different areas at 2% perturbation i-e (a) ten calculations & (b) fifty calculations.

Fig-2 displays the areas of freezing front cross-sectional from planes $z = z_0$, for $z_0 = 0.12, 0.22, 0.26, 0.28, 0.3$ and $0.32\,m$. For 10 and 50 measurements, the figure shows the exact and the reconstructed positions with the perturbation at 2%. Here the "e%" (mean relative error) is 0.083% & 0.080% related to the reconstruction of the freezing front, whereas it minimized to 0.030% for 100 measurements. For correct data freezing front's, reconstruction error, position remain less than 0.0014%.

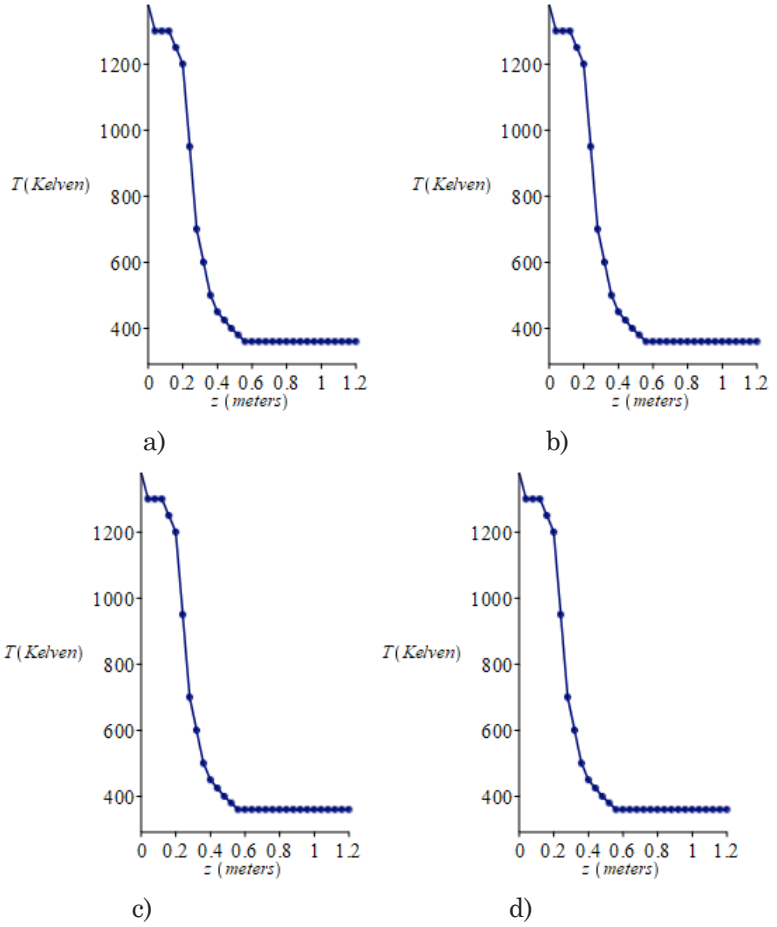

Figure 3. The solid line shows the Exact and dotted line shows reconstructed temperature values at the calculated points of 2% perturbation i-e 10 computations "(number of diagrams related to the number of sensors)".

In Fig-3, the correct and regenerated temperature distribution values appeared progressively using 4 measurement points in the input data weighed down by 2% error and the same of ten measurements.

Here, the topmost certain error is 1.65 K and mean absolute error is 0.27 K. The optimal and mean relative error of the recreation of temperature at the calculated points are 0.33% & 0.11% respectively. The reconstruction errors of temperature decreased by raising the number of calculations and accordingly, for 100 measurements the optimal and mean relative error is equal to $0.68 \& 0.09\ K$ and the optimal and mean relative error are $0.17\% \& 0.05\%$. The errors can be smaller for the starting data weighed down by lesser perturbations.

5 CONCLUSIONS

Here we discussed the problem of stabilizing the cooling conditions with two cooling zones; the first (basic one) and the second one, inside a 3D continuous-casting procedure. Given analysis presented by name of inverse Stefan problem, whereas it contained recreating a function which shows the boundary conditions while temperature estimations accepted at chosen positions into area examined. In numeric computations, we utilized the alternating phase truncation technique to determine the solution related to the inverse problem and 2 artificial intelligence algorithms that are ACO and PSO, to reduce the functional error.

Results displayed that for un-weighted input data, due to supposed termination of the numerical process of function that displayed the cooling conditions "(heat flux and heat transfer coefficient)" recreated by a small error. Minimizing the number of control points in the correct intake data didn't affect any big disturbances in the regenerated boundary conditions. This analysis shows, the correct input data troubled by assumed "(computational errors)" utilizing pseudo arbitrary numbers deriving out a normal distribution. The computations performed utilizing slight troubles (perturbations) with exact and different values. The outputs acquired, accepted free during disturbances ("perturbations") placed. It showed that errors in the recreated cooling conditions rely upon the weighted

information were commonly shorter than the intake errors. A part of the coefficients was re-established with errors bigger than information, however just for the smallest control point's values. But these reproduction errors were still admissible, particularly if we think about the errors in temperature description for a given state. Effects of temperature for described cases studied were recreated affirmatively.

The computations additionally demonstrated the results acquired by progressive iterations of the artificial intelligence (AI) algorithms had fundamentally the same, which had affirmed from short values of S.D "standard deviation". Given that correctness of acquired outputs, the utilization of optimization algorithms approximately the same. The benefit of the "ABC" algorithm for executing the analysis studied precisely just when it distinguished the duration needed for the calculations of algorithms. In addition, the operated counts, for which just a part of the outcomes was introduced in this investigation, showed the stabilizing of the given method regarding the input data errors and as far as the number of control points, along these lines affirming the convenience of the suggested methodology.

To quicken the suggested strategies, we intend to parallel the algorithms and want to build a hybrid algorithm in the future. We intend to consolidate the benefits of the organically propelled algorithm and classical optimization algorithms, whereas organically propelled algorithm will decide the beginning stage (which ought to be very near the required global problem) utilized by the traditional algorithm, along these lines enhancing the outcomes acquired.

Author Contributions:

Conceptualization, Muhammad Naeem and Naveed Sheikh; Formal analysis, Muhammad Naeem, Muhammad Asif and Durdana Munir; Writing – original draft, Naveed Sheikh, Mudassar Iqbal and Muhammad Naeem; Writing – review & editing, Muhammad Naeem, Mudassar Iqbal and Samina Naz.

REFERENCES

1) Binder, A., Engl, H. W., & Vessella, S. (1990). Some inverse problems for a nonlinear parabolic equation connected with continuous casting of steel: Stability estimates and regularization∗. Numerical functional analysis and optimization, 11(7-8), 643-671.
2) Chakraborti, N., Gupta, R. S. P., & Tiwari, T. K. (2003). Optimisation of continuous casting process using genetic algorithms: studies of spray and radiation cooling regions. Ironmaking & steelmaking, 30(4), 273-278.
3) Chakraborti, N., Kumar, R., & Jain, D. (2001). A study of the continuous casting mold using a pareto-converging genetic algorithm. Applied Mathematical Modelling, 25(4), 287-297.
4) Cheung, N., & Garcia, A. (2001). The use of a heuristic search technique for the optimization of quality of steel billets produced by continuous casting. Engineering Applications of Artificial Intelligence, 14(2), 229-238.
5) Dorigo, M., & Stützle, T. (2003). The ant colony optimization metaheuristic: Algorithms, applications, and advances. In Handbook of metaheuristics (pp. 250-285). Springer US.
6) Engl, H. W, & Langthaler, T. (1985). Numerical solution of an inverse problem connected with continuous casting of steel. Journal of Operations Research, 29 (6), B185-B199.
7) Engl, H. W., Langthaler, D. I. T., & Manselli, P. (1987). On an inverse problem for a nonlinear heat equation connected with continuous casting of steel. In Optimal Control of Partial Differential Equations II: Theory and Applications (pp. 67-89). Birkhäuser Basel.
8) Hetmaniok, D. Słota, A. Zielonka, (2012) Application of swarm intelligence algorithms in solving the inverse heat conduction problem, Comput. Assisted Meth. Eng. Sci. 19 361–367.
9) Hetmaniok, E., Słota, D., Zielonka, A., & Pleszczyński, M. (2013, June). Inverse continuous casting problem solved by applying the artificial bee colony algorithm. In International Conference on Artificial Intelligence and Soft Computing (pp. 431-440). Springer Berlin Heidelberg.
10) Hetmaniok, E., Słota, D., & Zielonka, A. (2015). Restoration of

the cooling conditions in a three-dimensional continuous casting process using artificial intelligence algorithms. Applied Mathematical Modelling, 39(16), 4797-4807.

11) Karaboga, D., & Basturk, B. (2007). A powerful and efficient algorithm for numerical function optimization: artificial bee colony (ABC) algorithm. Journal of global optimization, 39(3), 459-471.
12) Nawrat, A., &Skorek, J. (2005). Inverse approach and sensitivity analysis for identification of ingot-mould thermal resistance in continuous casting of metals. International Journal of Computational Fluid Dynamics, 19(6), 429-436.
13) Nowak, I., Smolka, J., & Nowak, A. J. (2010). An effective 3-D inverse procedure to retrieve cooling conditions in an aluminium alloy continuous casting problem. Applied Thermal Engineering, 30(10), 1140-1151.
14) O'Mahoney, D., & Browne, D. J. (2000). Use of experiment and an inverse method to study interface heat transfer during solidification in the investment casting process. Experimental Thermal and Fluid Science, 22(3), 111-122.
15) Rogers,J.C.W. Berger,A.E. Ciment,M. (1979). The alternating phase truncation method for numerical solution of a Stefan problem, SIAM J. Numer. Anal. 16(4) 563–587.
16) Santos, C. A., Spim, J. A., Ierardi, M. C., & Garcia, A. (2002). The use of artificial intelligence technique for the optimisation of process parameters used in the continuous casting of steel. Applied Mathematical Modelling, 26(11), 1077-1092.
17) Santos, C. A., Spim, J. A., & Garcia, A. (2003). Mathematical modeling and optimization strategies (genetic algorithm and knowledge base) applied to the continuous casting of steel. Engineering Applications of Artificial Intelligence, 16(5), 511-527.
18) Słota, D. (2008). Solving the inverse Stefan design problem using genetic algorithms. Inverse Problems in Science and Engineering, 16(7), 829-846.
19) Słota, D. (2009). Identification of the cooling condition in 2-D and 3-D continuous casting processes. Numerical Heat Transfer, Part B: Fundamentals, 55(2), 155-176.
20) Słota, D. (2011). Restoring boundary conditions in the

solidification of pure metals. Computers & structures, 89(1), 48-54.

21) Santos, C. A., Garcia, A., Frick, C. R., &Spim, J. A. (2006). Evaluation of heat transfer coefficients along the secondary cooling zones in the continuous casting of steel billets. Inverse Problems in Science and Engineering, 14(6), 687